

# Diagnostic performance of imaging criteria for distinguishing autoimmune cholangiopathy from primary sclerosing cholangitis and bile duct malignancy

Carly S. Gardner,<sup>1</sup> Mustafa R. Bashir,<sup>2,3</sup> Daniele Marin,<sup>2</sup> Rendon C. Nelson,<sup>2</sup> Kingshuk Roy Choudhury,<sup>2</sup> Lisa M. Ho<sup>2</sup>

<sup>1</sup>Department of Radiology, Baylor College of Medicine, One Baylor Plaza-BCM360, Houston, TX, USA

<sup>2</sup>Department of Radiology, Duke University Medical Center, Box 3808, Durham, NC, USA

<sup>3</sup>Center for Advanced Magnetic Resonance Development, Duke University Medical Center, Durham, NC, USA

## Abstract

**Objective:** To determine the diagnostic performance of imaging criteria for distinguishing Ig-G4-associated autoimmune cholangiopathy (IAC) from primary sclerosing cholangitis (PSC) and bile duct malignancy.

**Methods:** A medical records search between January 2008 and October 2013 identified 10 patients (8 M, 2 F, mean age 61 years, range 34–82) with a clinical diagnosis of IAC. Fifteen cases of PSC (6 M, 9 F, mean age 50, range 22–65) and 15 cases of biliary malignancy (7 M, 8 F, mean age 65, range 48–84) were randomly selected for comparative analysis. Three abdominal radiologists independently reviewed MRI with MRCP ( $n = 32$ ) or CT ( $n = 8$ ) and ERCP ( $n = 8$ ) for the following IAC imaging predictors: single-wall bile duct thickness  $>2.5$  mm, continuous biliary involvement, gallbladder involvement, liver disease, peribiliary mass, or pancreatic and renal abnormalities. Each radiologist provided an imaging-based diagnosis (IAC, PSC, or cancer). Imaging predictor sensitivity, specificity, accuracy, and association with IAC using Fisher's exact test. Inter-reader agreement determined using Fleiss' kappa statistics.

**Results:** For diagnosis of IAC, sensitivities and specificities were high (70–93%). Pancreatic abnormality was strongest predictor for distinguishing IAC from PSC and cancer, with high diagnostic performance (70–80% sensitivity, 87–97% specificity), significant association ( $p < 0.01$ ), and moderate inter-reader agreement ( $\kappa = 0.59$ ). Continuous biliary involvement was moder-

ately predictive (50–100% sensitivity, 53–83% specificity) and trended toward significant association in distinguishing from PSC ( $p = 0.01$ – $0.19$ ), but less from cancer ( $p = 0.06$ – $0.62$ ).

**Conclusion:** It remains difficult to distinguish IAC from PSC or bile duct malignancy based on imaging features alone. The presence of pancreatic abnormalities, including peripancreatic rind, atrophy, abnormal enhancement, or T2 signal intensity, strongly favors a diagnosis of IAC.

**Key words:** Autoimmune cholangiopathy—IgG4—Primary sclerosing cholangitis—Cholangiocarcinoma

Autoimmune cholangiopathy or IgG4-associated autoimmune cholangiopathy (IAC) [1] is an emerging diagnosis that can lead to significant morbidity if not recognized and treated appropriately. Because this disease is a relatively new clinical entity, consensus for defining this condition is still being developed and often involves a combination of clinical, pathologic, and imaging features [2].

The patient presentation with IAC is variable, ranging from asymptomatic to liver enzyme abnormalities, jaundice, and weight loss. Generally, patients with this disease have biliary strictures, and most, though not all, have elevated serum IgG4 levels [1]. IAC is most commonly associated not only with autoimmune pancreatitis (92–95%), but can also be seen alone or with involvement of other organs, including the kidney (26%), retroperitoneum (9%), salivary gland (6%), lymph nodes (4%),

and lung (4%) [3–6]. The biliary tree is in fact the most common extrapancreatic site of IgG4-mediated disease [7].

IAC almost universally involves the extrahepatic bile ducts, which makes imaging a valuable tool in the detection and evaluation of its progression [8]. However, IAC shares some imaging characteristics with primary sclerosing cholangitis (PSC) [9]. Distinguishing between these two entities is important because IAC responds well to corticosteroid therapy while PSC usually does not [9]. A recent study by Tokala et al. [10] proposed specific imaging criteria for differentiating IAC from primary sclerosing cholangitis (PSC) or other autoimmune liver diseases. One limitation of their study was the use of consensus reader analysis in a non-independent population, which led to observational results rather than an evaluation of diagnostic accuracy and performance.

IAC can also be difficult to distinguish from central bile duct malignancy. Bile duct wall thickening and peribiliary inflammatory pseudomasses are two well-described characteristics of IAC, which can simulate cholangiocarcinoma or other bile duct malignancies [11, 12]. Thus, identifying imaging characteristics which distinguish IAC from biliary tract malignancy is important in order to avoid making an incorrect diagnosis that could lead to unnecessary surgery or other procedures.

The purpose of our study is to assess the diagnostic performance of specific imaging criteria in differentiating IAC from PSC and biliary duct malignancy. These imaging criteria were derived from previous studies which have indicated that they have the potential to be strong predictors for IAC [10–12].

## Materials and methods

### *Patients*

This retrospective study was approved by the institutional research board and the requirement for informed consent was waived. Eligible subjects were identified by a medical records database search of CT or MRI reports between January 1, 2008 and October 31, 2013. The initial medical records search used the key words “IgG4 cholangiopathy,” “IgG4,” “cholangiopathy,” and “autoimmune cholangiopathy.” Thirty-four imaging reports (CT or MRI) were identified using these keywords and ten patients (8 males, 2 females, mean age 61 years, range 34–82 years) were identified with a diagnosis of autoimmune cholangiopathy based on our reference standard (below) who also had undergone either a contrast-enhanced MRI with magnetic resonance cholangiopancreatography (MRCP)  $n = 7$ , or a contrast-enhanced CT and endoscopic retrograde cholangiopancreatogram (ERCP)  $n = 3$ .

For comparative analysis, two additional searches were performed during the same time period to identify patients with PSC and biliary malignancy. The second

search used the keywords “primary sclerosing cholangitis” to identify patients with PSC. Three hundred and twenty-five imaging reports (CT or MRI) were identified using these keywords and fifteen patients (6 males, 9 females, mean age 50, range 22–65) with a diagnosis of PSC (based on our reference standard, below) that met our imaging requirements were randomly selected for inclusion in our study. All PSC patients were required to have a contrast-enhanced MRI with MRCP ( $n = 15$ ) or contrast-enhanced CT and ERCP ( $n = 0$ ). Lastly, the third search using keywords “cholangiocarcinoma” or “biliary tumor” was used to identify patients from a radiology database, with pathologically proven biliary malignancy. Nine hundred and forty-four patients were identified using these keywords and fifteen patients (7 male, 8 females, mean age 65, range 48–84) with biliary tract malignancy (based on our reference standard, below) that met our imaging requirements were randomly selected for inclusion in our study. Each of these patients had either a contrast-enhanced MRI with MRCP ( $n = 10$ ) or a contrast-enhanced CT and an ERCP ( $n = 5$ ). The final study group consisted of 10 patients with IAC, 15 patients with PSC, and 15 patients with biliary tract malignancy.

### *Reference standard*

Diagnostic criteria from The American Association for the Study of Liver Diseases [13] were used for the diagnosis of PSC ( $n = 15$ ). The diagnosis of IAC was made by using the Mayo Clinic HISORt (histology, imaging findings, serology, other organ involvement, and response to steroid treatment) criteria and applying the algorithm for diagnosis and management of IAC proposed by Ghazale et al. [5, 14, 15]. Table 1 lists the ten patients identified with IAC and the diagnostic criteria used to confirm their diagnosis. The diagnosis of biliary tract malignancy was established by surgical biopsy ( $n = 4$ ), liver biopsy ( $n = 7$ ), endoscopic bile duct biopsy ( $n = 2$ ), and percutaneous hepatic hilar node biopsy ( $n = 2$ ). The final pathologic diagnoses for this subgroup were cholangiocarcinoma ( $n = 11$ ), diffuse large B cell lymphoma involving the bile ducts ( $n = 1$ ), and biliary tract metastasis (colon, pulmonary and breast primary,  $n = 3$ ).

### *Imaging protocol*

MRI examinations had been performed at either 1.5 Tesla (Magnetom Avanto, Siemens Healthcare USA,  $n = 15$ ; Signa HDx, GE Healthcare,  $n = 6$ ) or 3.0 Tesla (Magnetom Trio Tim, Siemens Healthcare USA,  $n = 3$ ; Magnetom Skyra, Siemens Healthcare USA,  $n = 7$ ; Magnetom Aero, Siemens Healthcare USA,  $n = 1$ ). In patients who had undergone MRI for their diagnostic testing, the first standard pancreaticobiliary MRI that

**Table 1.** Criteria for diagnosis of immunoglobulin G4-associated cholangitis (IAC) using Mayo HISORt criteria

Patient #	Histology <sup>a</sup>	Imaging <sup>b</sup>	Serology mg/dL <sup>c</sup>	Other organ involvement <sup>d</sup>	Response to steroids <sup>e</sup>	Meets criteria <sup>f</sup>
1	Surgical pancreas specimen positive	Extrahepatic bile duct stricture	30	Pancreas	Marked improvement	Yes
2	Core ampullary biopsy negative	Intra and extrahepatic bile duct strictures	456	Pancreas	Complete resolution	Yes
3	Core pancreas biopsy negative	Extrahepatic stricture	234	Pancreas	Marked improvement	Yes
4	Core liver biopsy positive	Intra and extrahepatic strictures	Negative <sup>g</sup>	Lymph node	Marked improvement	Yes
5	Core pancreas biopsy positive	Extrahepatic stricture	195	Pancreas	Complete resolution	Yes
6	Core liver biopsy positive	Intrahepatic strictures	None	None	Complete resolution	Yes
7	Core pancreas biopsy negative	Extrahepatic stricture	508	Pancreas	Complete resolution	Yes
8	Core (athrectomy) bile duct biopsy positive	Extrahepatic stricture	163	Pancreas	Unknown, no follow-up	Yes
9	Core liver biopsy positive	Extrahepatic stricture	17	None	Complete resolution	Yes
10	Core ampullary biopsy positive	Intra and Extrahepatic strictures	39.4	Pancreas	Unknown, no follow-up	Yes

<sup>a</sup> Histology shows periductal lymphoplasmacytic infiltrate with >10 IgG4-positive cells/hpf with associated obliterative phlebitis and storiform fibrosis

<sup>b</sup> One or more strictures involving the intrahepatic, proximal extrahepatic, or intrapancreatic bile ducts; fleeting/migrating biliary strictures

<sup>c</sup> Increased levels of serum IgG4 (normal, 2.4–121 mg/dL)

<sup>d</sup> Evidence for IgG4-related systemic disease involving pancreas, retroperitoneal fibrosis, renal lesions, and/or salivary/lacrimal gland

<sup>e</sup> Normalization of liver enzyme levels or marked improvement or resolution of stricture

<sup>f</sup> Diagnosis of IAC based on algorithm published by Ghazale et al. [5] and Chari et al. [15]

<sup>g</sup> Serology results reported as negative in medical record for this patient but exact value is not available

**Table 2.** Sample MR pulse sequences at 1.5 and 3T

Parameter	T1w dual echo	T1w unenhanced	T1w contrast enhanced	T2w respiratory triggered
<b>1.5 T</b>				
Repetition time (ms)	5.2–7.5	3.2–5.1	3.2–5.1	6800–12,900
Echo time (ms)	2.2–2.4/4.4–4.8	1.5–2.3	1.5–2.3	87–90
Flip angle (°)	10–12	10–12	10–12	90–150
Slice thickness (mm)	3–4 mm	4–7	4–7	5
Reconstruction interval (mm)	2–3 mm	3.5–4	3.5–4	6–7
Acquisition matrix	256 × 192	256 × 192	256 × 192	256–384 × 179–224
Acceleration factor	2	2	2	2
Signal averages				2
<b>3.0 T</b>				
Repetition time (ms)	3.9–4.5	3.9–4.5	3.9–4.5	7100–10,900
Echo time (ms)	1.2–1.3/ 2.4–2.6	1.2–1.3	1.2–1.3	89–102
Flip angle (degrees)	9–12	9–12	9–12	90–140
Slice thickness (mm)	2–4	2–4	2–4	5
Reconstruction interval (mm)	2	2	2	6–7
Acquisition matrix	256–320 × 192	256–320 × 192	256–320 × 192	320–384 × 224–320
Acceleration factor	2	2	2	2
Signal averages				2

included MRCP and gadolinium-based contrast enhancement was selected for review. Contrast agents used included the following: 0.1 mL/kg gadobenate dimeglumine (Multihance, Bracco Diagnostics, Inc., Princeton, NJ),  $n = 17$ ; or 10 mL dose of gadoxetate disodium (Eovist, Bayer Healthcare, Inc., Wayne, NJ),  $n = 15$ . Note that this dose of gadoxetate disodium is based on our standard clinical practice and maximizes arterial enhancement [16]. All MRI protocols included the following pulse sequences: coronal T2-weighted half-Fourier acquisition single-shot turbo spin echo (HASTE), axial in-phase and opposed-phase gradient recalled echo, axial respiratory triggered and fat-suppressed T2-weighted fast spin echo, MRCP, axial T1-weighted 3D spoiled gradient echo (precontrast and dynamic post-contrast including triple phase arterial, portal venous, and equilibrium).

Additional 20 min delayed phase images were acquired obtained with gadoxetate disodium only with axial and coronal T1-weighted 3D spoiled gradient echo imaging [16]. Protocol details for MRI pulse sequences used are listed on Tables 2, 3.

CT was performed using 64-MDCT scanner (Somatom Definition, Siemens Healthcare, Inc., Forchheim, Germany,  $n = 4$ ; or LightSpeed VCT, GE Healthcare, Inc., Waukesha, Wisconsin,  $n = 3$ ) or 16-MDCT scanner (GE LightSpeed 16,  $n = 1$ ). In patients who had undergone CT for their diagnostic testing, the first standard protocol abdomino-pelvic CT with intravenous contrast material was selected for review and paired with the first diagnostic ERCP. For all CT studies, 150 mL of iopamidol (Isovue 300, 300 mgI/mL, Bracco Diagnostics Inc), were injected intravenously at 3 mL/second via an

**Table 3.** Sample MRCP protocols for 1.5 T and 3.0 T

Parameter	2D thick slab MRCP	3D thin slice MRCP
Relaxation time (ms)	2800–4500	3700–6300
Echo time (ms)	496–762	668–710
Flip angle (°)	90	90
Slice thickness (mm)	5–6 cm	1 mm
Slices/volume	1	60
Matrix	384 × 384	384 × 384
Resolution (mm × mm)	0.8–0.9 × 0.8–0.9	0.8–1.0 × 0.8–1.0
Parallel acceleration factor	3	3
Signal averages	1	2
Bandwidth (Hz/px)	150–385	320–362

**Table 4.** Summary of autoimmune cholangiopathy imaging predictors

Predictor of Autoimmune Cholangiopathy	Description
1. Single bile duct wall thickness >2.5 mm	(Outer–inner diameter)/2; Assessed on contrast-enhanced MR images acquired during equilibrium or portal venous phase or on contrast-enhanced CT during portal phase imaging
2. Continuous biliary involvement	Long segment stricture with undulating thickened wall and/or abnormally enhancing wall (i.e., no normal intervening bile duct)
3. Gallbladder involvement	Enhancing or thickened wall
4. Absence of liver abnormality	Absence of lobar atrophy or hypertrophy, absence of cirrhosis, no portal vein thrombosis
5. Peribiliary mass	Focal or diffuse mass next to biliary duct
6. Pancreatic abnormality	MRI: abnormal signal intensity on T1 or T2-weighted images; focal or diffuse atrophy; areas of abnormal enhancement, peripancreatic rind of tissue (halo)
7. Renal abnormalities	Cortical nodules; wedge-shaped cortical lesions, peri-renal fibrosis

**Table 5.** Sensitivity, specificity, and accuracy for diagnosis of autoimmune cholangiopathy

Radiologist	IAC vs. PSC or Cancer	Sensitivity	Specificity	Accuracy
R1	Overall	70% (7/10)	86% (26/30)	83% (33/40)
R2	Overall	70% (7/10)	93% (23/30)	88% (35/40)
R3	Overall	90% (9/10)	77% (23/30)	80% (32/40)
R1	PSC	70% (7/10)	87% (13/15)	80% (20/25)
R2	PSC	70% (7/10)	100% (15/15)	88% (22/25)
R3	PSC	90% (9/10)	80% (12/15)	84% (21/25)
R1	CA	70% (7/10)	87% (13/15)	80% (20/25)
R2	CA	70% (7/10)	87% (13/15)	80% (20/25)
R3	CA	90% (9/10)	73% (11/15)	80% (20/25)

**Table 6.** Imaging predictor sensitivity and specificity for autoimmune cholangiopathy

Predictors	Sensitivity			Specificity		
	R1	R2	R3	R1	R2	R3
CBD >2.5 mm	80% (8/10)	60% (6/10)	90% (9/10)	43% (13/30)	50% (15/30)	57% (17/30)
Continuous biliary involvement	90% (9/10)	100% (10/10)	50% (5/10)	53% (16/30)	60% (18/30)	83% (25/30)
Gallbladder involvement	38% (3/8)	40% (4/10)	25% (2/8)	73% (16/22)	81% (18/22)	63% (14/22)
Absence of liver disease	90% (9/10)	90% (9/10)	60% (6/10)	23% (7/30)	33% (10/30)	43% (13/30)
Peribiliary mass	60% (6/10)	10% (1/10)	20% (2/10)	63% (19/30)	67% (20/30)	63% (19/30)
Pancreas abnormality	<b>80% (8/10)</b>	<b>70% (7/10)</b>	<b>70% (7/10)</b>	<b>87% (26/30)</b>	<b>93% (28/30)</b>	<b>97% (29/30)</b>
Renal abnormality	0% (0/10)	10% (1/10)	0% (0/10)	100% (30/30)	100% (30/30)	97% (29/30)
Multivariate (Tree) analysis	80% (8/10)	70% (7/10)	70% (7/10)	87% (26/30)	93% (28/30)	97% (29/30)
Linear discriminant analysis	70% (7/10)	80% (8/10)	70% (7/10)	87% (26/30)	90% (18/30)	93% (28/30)

arm vein. All CT scans were performed using a two-phase liver protocol which included a late hepatic arterial phase (based on bolus tracking software from the supraceliac abdominal aorta), and portal venous phase (obtained 40 s after the end of the hepatic arterial phase). Images were acquired using the following technique: 120

kVp, variable mA (noise index of 15 HU on the GE systems, Care Dose 4d with reference mA of 250 mA on Siemens systems) and 0.5 s gantry rotation time. Contiguous images were reconstructed in the axial plane at 5 mm thickness in the hepatic arterial and portal venous phases. Contiguous images were also reconstructed in the

**Table 7.** Association of imaging predictor for autoimmune cholangiopathy (IAC) vs. non-IAC (primary sclerosing cholangitis or biliary tract malignancy)

Reader (R)	IAC vs. PSC or CA	CBD >2.5 mm	Continuous biliary involvement	GB involve-ment	Absence of liver abnormality	Peribiliary mass	Panc abnormality	Renal abnormality
R1	PSC	0.23	0.01	0.62	0.09	0.01	0.01	1.00
R2	PSC	0.12	0.01	0.03	0.02	0.40	0.01	0.40
R3	PSC	0.01	0.19	0.21	0.24	0.15	0.01	1.00
R1	CA	1.00	0.62	1.00	0.40	0.67	0.01	1.00
R2	CA	0.67	0.06	0.34	1.00	0.01 <sup>a</sup>	0.01	0.40
R3	CA	0.18	0.08	0.17	0.38	0.01 <sup>a</sup>	0.01	1.00

Fisher's exact test, all values in table represent  $p$  values with  $p < 0.05$  indicating a statistically significant association

<sup>a</sup> These results reflect a significant association of peribiliary mass with bile duct malignancy compared with IAC

coronal plane in the portal venous phase data sets at 3 mm thickness.

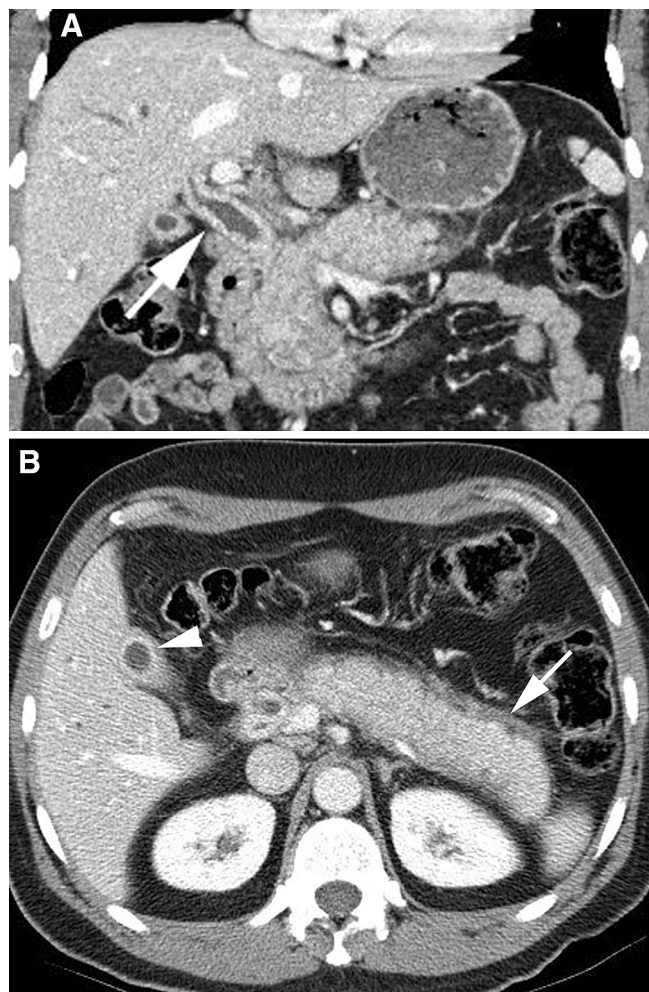


**Fig. 1.** 56-year-old man with IAC. **A** Coronal contrast-enhanced CT demonstrates a dilated and thick-walled common bile duct (*arrow*) and mild intrahepatic biliary ductal dilation. Pancreatic head and body appear diffusely enlarged with surrounding inflammatory change. **B** Axial contrast-enhanced CT in the same patient demonstrates diffusely enlarged and hypo-enhancing pancreas body and tail with peripancreatic rim of low attenuation (*arrow*) consistent with diagnosis of autoimmune pancreatitis. Also note, diffuse thickening of the gallbladder wall (*arrowhead*).

### Review of imaging

All studies of IAC, PSC, and biliary malignancy were randomized. Three fellowship-trained abdominal radiologists, (experience 5, 7, and 29 years) reviewed the imaging studies independently and blinded to any clinical data. MRI with MRCP ( $n = 22$ ) and CT paired with ERCP ( $n = 8$ ) were scored for the presence or the absence of the following imaging predictors of IAC [10]: (1) single-wall bile duct thickness >2.5 mm; (2) continuous biliary involvement, (3) gallbladder involvement, (4) absence of chronic liver disease, (5) peribiliary mass, (6) pancreatic abnormalities, and (7) renal abnormalities. Detailed descriptions of each imaging predictor were provided to the readers prior to image review and are presented in Table 4.

Each radiologist provided a final imaging-based diagnosis of IAC, PSC, or biliary tract malignancy and a confidence level, 1–5, for that diagnosis (1 = unsure, low confidence <10%, 2 = slightly favor one diagnosis, 10–39% confidence, 3 = moderately favor one diagnosis, 40–59% confidence, 4 = strongly favor one diagnosis, 60–90% confidence, 5 = almost certain of diagnosis, >90% confidence).

### Statistical analysis

Diagnostic performance, including sensitivity, specificity, and accuracy for distinguishing IAC from PSC or biliary

**Table 8.** Inter-reader agreement for predictors

Predictors	$\kappa$
CBD >2.5 mm	0.19
Continuous biliary involvement	0.19
Gallbladder involvement	0.26
Liver abnormality	0.48
Peribiliary mass	0.52
Pancreatic abnormality	0.59

**Table 9.** Reader confidence level by diagnosis accuracy

Diagnosis accuracy	Confidence value	Std. Error	$p$ value
Incorrect	3.22	0.23	n/a
Correct	3.92	0.22	0.002

malignancy, was determined for each radiologist. Sensitivity and specificity were determined for the seven imaging predictors for each of the three radiologists. In addition, a multivariate tree analysis and linear discriminant analysis were performed to determine if a combination of predictors performed more strongly than individual predictors. The association of each imaging predictor for IAC compared with PSC or biliary tract malignancy was determined by using Fisher's exact test,  $p < 0.05$  to indicate a significant association. Inter-reader agreement was determined using Fleiss's kappa statistics, with less than 0 equal to poor agreement, 0.00–0.40 slight to fair agreement, 0.4–0.6 moderate agree-

ment, 0.61–0.8 substantial agreement, and 0.81–1.0 almost perfect agreement. Mean radiologist confidence levels were compared between correct and incorrect diagnoses using a linear mixed model with reader-specific random effects and a fixed effect for correctness of diagnosis.

## Results

The overall sensitivity and specificity for establishing a diagnosis of IAC vs. PSC or biliary malignancy was moderate to high, with percent sensitivities of 70%, 70%, and 90% and percent specificities of 86%, 93%, and 77%, for radiologists 1, 2, and 3, respectively (Table 5).

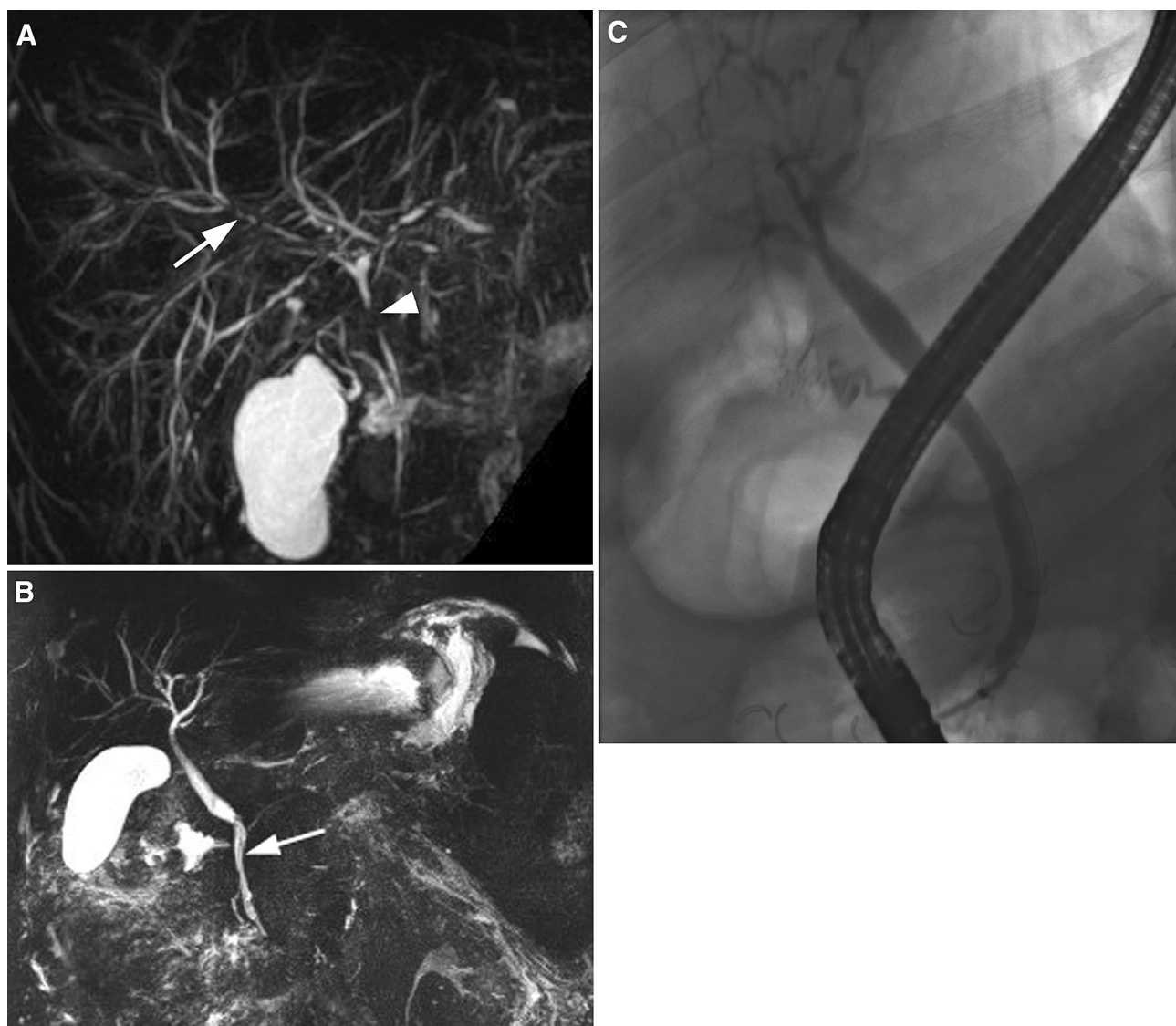


**Fig. 2.** Comparison of PSC and IAC. **A** 29-year-old man with PSC. MRCP demonstrates multiple short segment strictures of the intrahepatic (*arrow*) and extrahepatic (*arrowhead*) bile ducts. **B** 60-year-old man with IAC. MRCP demonstrates long segment distal biliary stricture (*arrow*)

without skip areas (continuous biliary involvement) which is characteristic of IAC. **C** 6 months later, following a course of steroids, endoscopic retrograde cholangiopancreatogram of same patient (**B**) demonstrates resolution of the common bile duct stricture.

Diagnostic accuracy was moderate, with percentage values of 83%, 88%, and 80%, for radiologists 1, 2, and 3, respectively. Higher diagnostic performance was demonstrated for distinguishing IAC from PSC, with specificity values of 87%, 100%, and 80% for radiologists 1, 2, and 3, respectively. By comparison, lower specificity was seen for distinguishing IAC from bile duct malignancy with values of 87%, 87%, and 73% for radiologists 1, 2, and 3, respectively.

Each imaging predictor was then assessed for its individual sensitivity and specificity for diagnosing IAC, as shown in Table 6. A pancreatic abnormality was the only imaging predictor with both high sensitivity (80%, 70%, 70%) and specificity (87%, 90%, 97%) for all radiologists 1, 2, and 3, respectively (Table 6, bold values). Multivariate analysis was performed by grouping individual imaging predictors using various combinations in an attempt to achieve increased sensitivity or specificity. No combination of imaging predictors, however, had higher performance than the presence of pancreatic abnormalities alone for the diagnosis of IAC. Common bile duct single-wall thickness greater than 2.5 mm had moderate-to-high sensitivity (80%, 60%, 90%) but only moderate specificity (43%, 50%, 57%), for radiologists 1, 2, and 3, respectively. Continuous biliary involvement had a wide range of sensitivities (90%, 100%, 50%) and specificities (53%, 60%, 83%) for radiologists 1, 2, and 3, respectively.

Imaging predictors were assessed for their ability to distinguish IAC vs. non-IAC (PSC or bile duct malig-

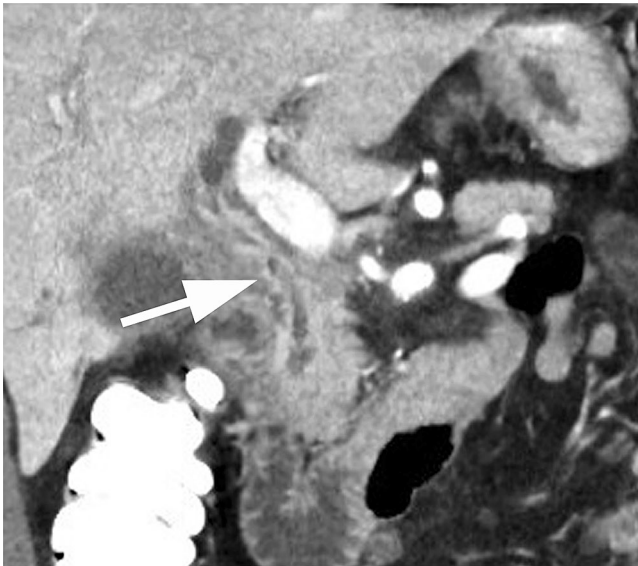


**Fig. 3.** 62-year-old woman with cholangiocarcinoma. Coronal contrast-enhanced CT demonstrates long segment common bile duct stricture with thickened and enhancing walls (*arrow*). The appearance of this malignant stricture is similar to the appearance of biliary strictures in autoimmune cholangiopathy.

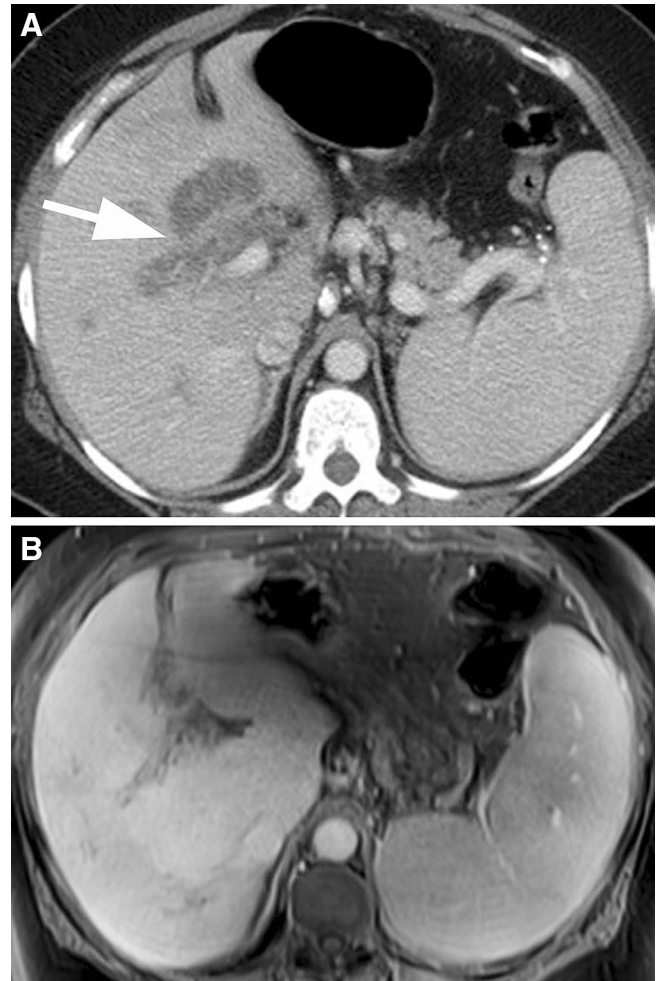


**Fig. 4.** 59-year-old woman with IAC and peribiliary pseudomass. **A** Axial contrast-enhanced CT shows an ill-defined mass (*arrow*) within the central liver, mimicking a cholangiocarcinoma. **B** Following a course of steroid therapy, the mass resolved on subsequent MR obtained 5 months later. Noted incidentally, interval portal vein thrombosis with cavernous transformation.

nancy), summarized in Table 7. The presence of pancreatic abnormalities was significantly associated with IAC over both PSC and bile duct malignancy for all three readers ( $p < 0.01$ ). Continuous biliary involvement rather than skip lesions was significantly associated with IAC over PSC for two out of three readers (reader 1 and 2,  $p < 0.01$ ; reader 3,  $p = 0.19$ ), but less helpful in predicting IAC over cancer for all three readers ( $p > 0.06$ ; see Fig. 1). Bile duct single-wall thickness  $> 2.5$  mm was significant in one reader for IAC over PSC ( $p < 0.01$ ), but not the other two readers ( $p > 0.12$ ). Moreover, bile duct wall thickness was not helpful at all for distinguishing IAC over cancer for all readers ( $p > 0.18$ ). The absence of liver abnormalities was significant or approached significance in predicting IAC over PSC in two out three readers ( $p = 0.02$  and

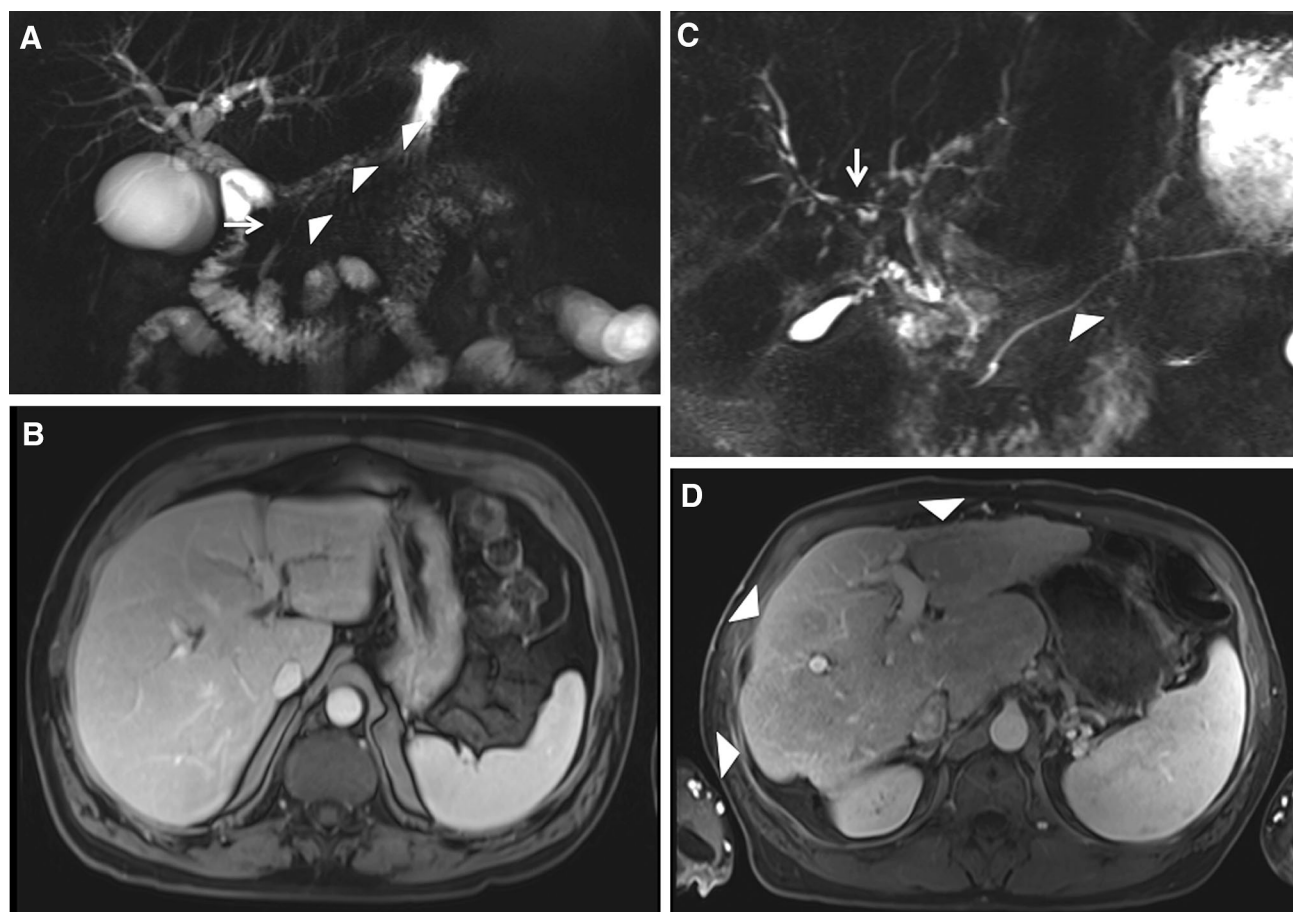


**Fig. 5.** Comparison of IAC and PSC. **A** 58-year-old man with IAC. MRCP demonstrates tight stricture in the mid to distal common bile duct (*arrow*). Note the mild narrowing and irregularity of the pancreatic duct (*arrowheads*) related to autoimmune pancreatitis. **B** Same patient as in **A**. Axial T1-weighted image of the liver during portal venous phase of contrast enhancement shows normal contour of the non-cir-

rhotic liver. **C** 57-year-old man with a history of PSC. MRCP image demonstrates multiple intrahepatic bile duct strictures (*arrow*) with skip areas. Note the normal appearance of the pancreatic duct (*arrowhead*). **D** Same patient as in image **C**. Axial T1-weighted image of the liver during the portal venous phase of contrast enhancement shows the lobulated contour of the cirrhotic liver (*arrowheads*).

0.09), but was not helpful in distinguishing IAC from bile duct malignancy ( $p > 0.38$ ). The presence of a peribiliary mass was more significantly associated with cancer than IAC in two out of three readers ( $p = 0.01, 0.01,$  and  $0.67$ ).

Moderate inter-reader agreement was demonstrated for identifying the presence of pancreatic abnormalities (0.59), liver abnormalities (0.48), and peribiliary mass (0.52) (Table 8). The remaining predictors demonstrated only slight-to-fair inter-reader agreement (0.19–0.26).

A statistically significant increase in mean confidence level of the three radiologists was demonstrated with correct diagnoses compared with incorrect diagnoses (Table 9,  $p = 0.002$ ).

## Discussion

In patients with biliary stricturing disease, the presence of concomitant pancreatic abnormalities favors a diag-

nosis of IAC over both PSC and biliary malignancy. Our results showed that pancreatic abnormalities, including focal and diffuse enlargement, T1-weighted signal hypointensity on MRI, severe atrophy, and a peripancreatic rind, demonstrated both moderately high sensitivity (70–80%) and specificity (87–97%) in diagnosing IAC (Fig. 1). This is in keeping with previous studies having large sample sizes, which found 92–95% association of IAC with autoimmune pancreatitis [11, 12]. In our study, we found that the presence of pancreatic abnormalities performed well for the diagnosis of IAC and were well agreed upon by readers. This reinforces its use as a reliable and generalizable imaging predictor.

Contiguous biliary involvement and bile duct wall thickening have been described in IAC, distinct from the skip lesions characterized by intervening segments of normal bile duct in PSC [17] (Fig. 2). This was confirmed in the recent Tokala study based on MRI examinations [10]. Our study, however, showed that although these



imaging features may be helpful in favoring IAC over PSC, they have a lesser role in differentiating IAC from malignancy. Both IAC and bile duct malignancy can have continuous biliary involvement and bile duct wall thickening (Fig. 3). The periductal and infiltrating nature of primary biliary malignancy and diffuse biliary involvement by metastatic disease and even lymphoma or leukemia [18, 19] may mimic the contiguous undulating involvement described as typical of IAC [20–26]. This observation has previously been made in a study by Kim et al. [25], who found that smooth margins and gradual undulating involvement were not specific for IAC, and were seen in up to 58% of patients with biliary malignancy. Periductal cholangiocarcinoma infiltrates along the bile duct wall and is associated with exuberant fibrosis [23, 24, 27], which may explain the similar imaging appearance. Moreover, a peribiliary mass can be seen in both biliary malignancy and IAC (Fig. 4) and is thus not a reliable imaging biomarker. In fact, for two of the three radiologists, the presence of a peribiliary mass was significantly associated with bile duct cancer rather than IAC, likely reflecting the potential nature of malignancy to invade adjacent structures. Misdiagnosis of biliary malignancy as IAC may lead to delayed or incorrect treatment. Furthermore, in our study, we found lower specificity and diagnostic accuracy for distinguishing IAC from bile duct malignancy compared with the relatively better diagnostic performance of distinguishing IAC from PSC.

The presence of liver abnormalities such as cirrhosis has also been suggested to support a diagnosis of PSC over IAC in patients with biliary strictures [10] (Fig. 5). Although a trend toward such an association was observed with our study, this finding was statistically significant for only one of three readers ( $p = 0.02, 0.09,$  and  $0.24$ ). This may be because the presence of lobar redistribution and cirrhosis is only seen in 55–68% [28] of patients with PSC and is only typically seen in the later stages of the disease [29].

We acknowledge several limitations in our study. First, we had a small sample size of IAC patients. IAC is uncommon and the proportion of IAC patients was matched with an similar number of patients with PSC and biliary malignancy for comparative analysis, allowing for optimal assessment of potential imaging criteria of a rare though emerging disease. However, by limiting our study population in this way, the results may not reflect prevalence of disease or whether the diagnostic features can lead to false positive diagnoses in patients without disease. Second, the imaging techniques in our study varied. The majority of patients had an MRI with MRCP while others had CT with ERCP, and only about 2/3 of the MRIs included contrast-enhanced hepatobiliary phase imaging. Nonetheless, the combined imaging modalities allow for accurate diagnosis of the evaluated imaging features. Furthermore, this approach more clo-

sely reflects imaging variation in the real world and everyday imaging practice. Useful imaging predictors for IAC should be generalizable not only across disease entities but across imaging modalities. Another limitation of this study is the use of a hepatocellular contrast agent in five of the ten cases of patients with IAC. Hepatic uptake in the venous and delayed phases may mask enhancement of the bile duct wall and as a result the use of this agent may limit the ability for detection of findings specific to IAC, such as bile duct wall enhancement and thickening, continuous biliary involvement, and gallbladder wall abnormalities. The use of this agent may have contributed to the decreased statistical significance when comparing IAC with the other two disease processes. Another limitation of this study is the potential for selection bias. Because the IAC cases have been selected from a group of patients with the imaging reports suggesting IAC as a differential, these cases likely had imaging features in favor of IAC. The lack of inclusion of atypical cases of IAC may have altered the results of the study. Lastly, we did not factor in the presence or absence of other potential areas of IgG4-associated disease outside of the upper abdomen. For example, it is known that patients with IAC can also have involvement of the salivary glands and retroperitoneal fibrosis. Detecting disease in these areas may also contribute to the accuracy of diagnosis in clinical practice, but these areas of the body were not included in our study. Nevertheless, these sites of IgG4-associated disease are usually found in patients who already have pancreatic involvement, which was included in our study [1].

## Conclusion

In conclusion, our study evaluates the diagnostic performance of the most useful imaging criteria for distinguishing IAC from PSC and biliary malignancy. In patients with a biliary stricture, it remains difficult to distinguish IAC from PSC or biliary malignancy based on imaging features alone. However, the presence of pancreatic abnormalities strongly favors a diagnosis of IAC.

## References

1. Lindor KD (2011) Immunoglobulin g4-associated autoimmune cholangiopathy. *Gastroenterol Hepatol* 7:259–261
2. Nakazawa T, Naitoh I, Hayashi K, et al. (2013) Diagnosis of IgG4-related sclerosing cholangitis. *World J Gastroenterol* 19:7661–7670
3. Kamisawa T, Okamoto A (2008) IgG4-related sclerosing disease. *World J Gastroenterol* 14:3948–3955
4. Matsubayashi H, Uesaka K, Sugiura T, et al. (2014) IgG4-related sclerosing cholangitis without obvious pancreatic lesion: difficulty in differential diagnosis. *J Dig Dis* 15:394–403
5. Ghazale A, Chari ST, Zhang L, et al. (2008) Immunoglobulin G4-associated cholangitis: clinical profile and response to therapy. *Gastroenterology* 134:706–715
6. Nakazawa T, Naitoh I, Hayashi K, et al. (2012) Diagnostic criteria for IgG4-related sclerosing cholangitis based on cholangiographic classification. *J Gastroenterol* 47:79–87

7. Zen Y, Onodera M, Inoue D, et al. (2009) Retroperitoneal fibrosis: a clinicopathologic study with respect to immunoglobulin G4. *Am J Surg Pathol* 33:1833–1839
8. Naitoh I, Zen Y, Nakazawa T, et al. (2011) Small bile duct involvement in IgG4-related sclerosing cholangitis: liver biopsy and cholangiography correlation. *J Gastroenterol* 46:269–276
9. Nakazawa T, Ohara H, Sano H, et al. (2004) Cholangiography can discriminate sclerosing cholangitis with autoimmune pancreatitis from primary sclerosing cholangitis. *Gastrointest Endosc* 60:937–944
10. Tokala A, Khalili K, Menezes R, Hirschfield G, Jhaveri KS (2014) Comparative MRI analysis of morphologic patterns of bile duct disease in IgG4-related systemic disease versus primary sclerosing cholangitis. *AJR Am J Roentgenol* 202:536–543
11. Ahn KS, Kang KJ, Kim YH, et al. (2012) Inflammatory pseudotumors mimicking intrahepatic cholangiocarcinoma of the liver; IgG4-positivity and its clinical significance. *J Hepato-Biliary-Pancreat Sci* 19:405–412
12. Hamano H, Kawa S, Uehara T, et al. (2005) Immunoglobulin G4-related lymphoplasmacytic sclerosing cholangitis that mimics infiltrating hilar cholangiocarcinoma: part of a spectrum of autoimmune pancreatitis? *Gastrointest Endosc* 62:152–157
13. Chapman R, Fevery J, Kalloo A, et al. (2010) Diagnosis and management of primary sclerosing cholangitis. *Hepatology* 51:660–678
14. Chari ST (2007) Diagnosis of autoimmune pancreatitis using its five cardinal features: introducing the Mayo Clinic's HISORT criteria. *J Gastroenterol* 42(Suppl 18):39–41
15. Chari ST, Smyrk TC, Levy MJ, et al. (2006) Diagnosis of autoimmune pancreatitis: the Mayo Clinic experience. *Clin Gastroenterol Hepatol.* 4:1010–1016
16. Bashir MR, Gupta RT, Davenport MS, et al. (2013) Hepatocellular carcinoma in a North American population: does hepatobiliary MR imaging with Gd-EOB-DTPA improve sensitivity and confidence for diagnosis? *J Magn Reson Imaging* 37:398–406
17. MacCarty RL, LaRusso NF, Wiesner RH, Ludwig J (1983) Primary sclerosing cholangitis: findings on cholangiography and pancreatography. *Radiology* 149:39–44
18. Choi EK, Byun JH, Lee SJ, et al. (2007) Imaging findings of leukemic involvement of the pancreaticobiliary system in adults. *AJR Am J Roentgenol* 188:1589–1595
19. Mani H, Climent F, Colomo L, et al. (2010) Gall bladder and extrahepatic bile duct lymphomas: clinicopathological observations and biological implications. *Am J Surg Pathol* 34:1277–1286
20. Erkelens GW, Vlegaar FP, Lesterhuis W, van Buuren HR, van der Werf SD (1999) Sclerosing pancreato-cholangitis responsive to steroid therapy. *Lancet* 354:43–44
21. Hirano K, Shiratori Y, Komatsu Y, et al. (2003) Involvement of the biliary system in autoimmune pancreatitis: a follow-up study. *Clin Gastroenterol Hepatol* 1:453–464
22. Horiuchi A, Kawa S, Hamano H, et al. (2002) ERCP features in 27 patients with autoimmune pancreatitis. *Gastrointest Endosc* 55:494–499
23. Lim JH (2003) Cholangiocarcinoma: morphologic classification according to growth pattern and imaging findings. *AJR Am J Roentgenol* 181:819–827
24. Zen Y, Harada K, Sasaki M, et al. (2004) IgG4-related sclerosing cholangitis with and without hepatic inflammatory pseudotumor, and sclerosing pancreatitis-associated sclerosing cholangitis: do they belong to a spectrum of sclerosing pancreatitis? *Am J Surg Pathol* 28:1193–1203
25. Kim JH, Byun JH, Lee SJ, et al. (2012) Differential diagnosis of sclerosing cholangitis with autoimmune pancreatitis and periductal infiltrating cancer in the common bile duct at dynamic CT, endoscopic retrograde cholangiography and MR cholangiography. *Eur Radiol* 22:2502–2513
26. Park KW, Lim JH, Jang KT, Choi DW (2008) Autoimmune cholangitis mimicking periductal-infiltrating cholangiocarcinoma. *Abdom Imaging* 33:334–336
27. Lim JH, Park CK (2004) Pathology of cholangiocarcinoma. *Abdom Imaging* 29:540–547
28. Ito K, Mitchell DG, Outwater EK, Blasbalg R (1999) Primary sclerosing cholangitis: MR imaging features. *AJR Am J Roentgenol* 172:1527–1533
29. Campbell WL, Ferris JV, Holbert BL, Thaete FL, Baron RL (1998) Biliary tract carcinoma complicating primary sclerosing cholangitis: evaluation with CT, cholangiography, US, and MR imaging. *Radiology* 207:41–50